Impact of acquisition and analysis strategies on cortical depth-dependent fMRI

Supplementary Material

Impact of acquisition and analysis strategies on cortical depth-dependent fMRI.

Sriranga Kashyap, Dimo Ivanov, Martin Havlicek, Benedikt A. Poser, Kamil Uludag

Department of Cognitive Neuroscience, Maastricht University, Maastricht, The Netherlands

FIGURE S1: Reduced contrast flickering (left) and full contrast static (right) stimuli.

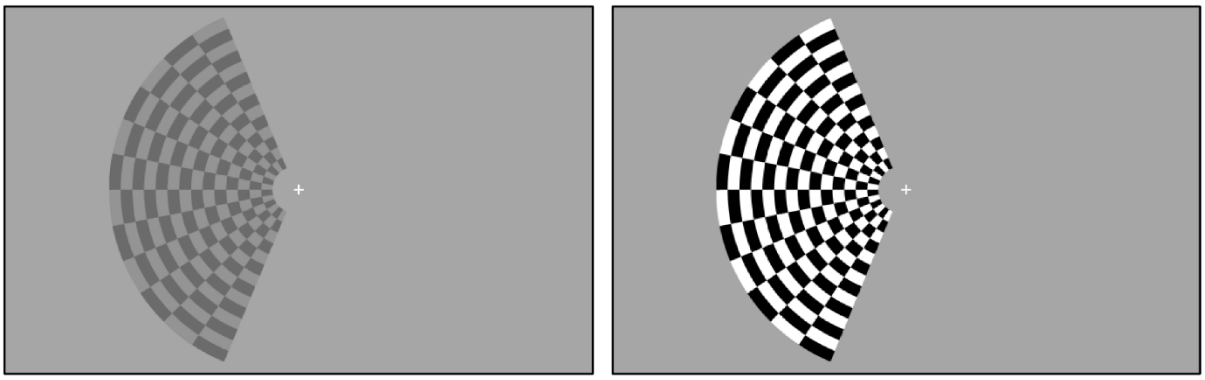

Flickering (~8 Hz, Michelson contrast 1/3) and static (Michelson contrast 1) checkerboard hemi-annuli created using PyschoPy.

FIGURE S2: MI-EPI contrast at different inversion times.

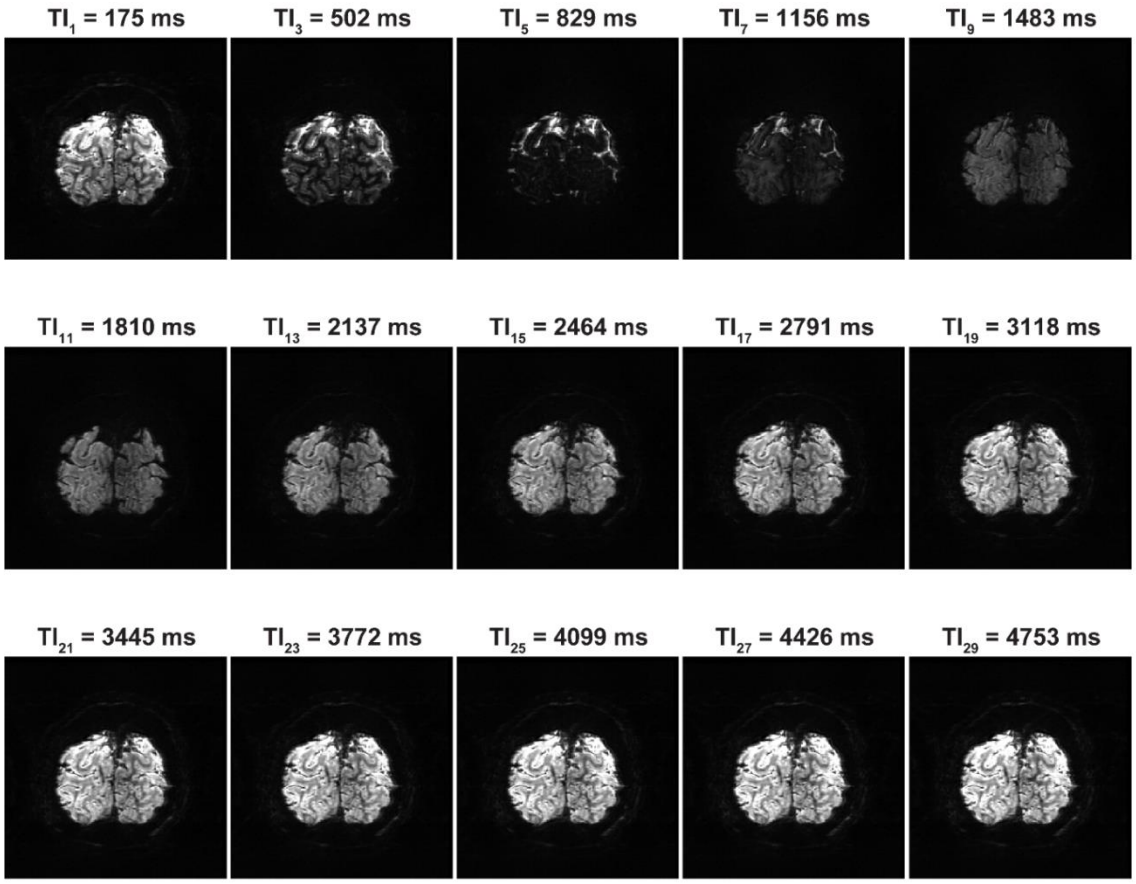

Contrast changes in the same slice from an example subject for 15 (out of 30) inversion times acquire with the MI-EPI procotol and used to compute the quantitative T_1 map.

FIGURE S3: Identification of venous voxels using the mean and temporal signal-to-noise (tSNR) maps from the functional data.

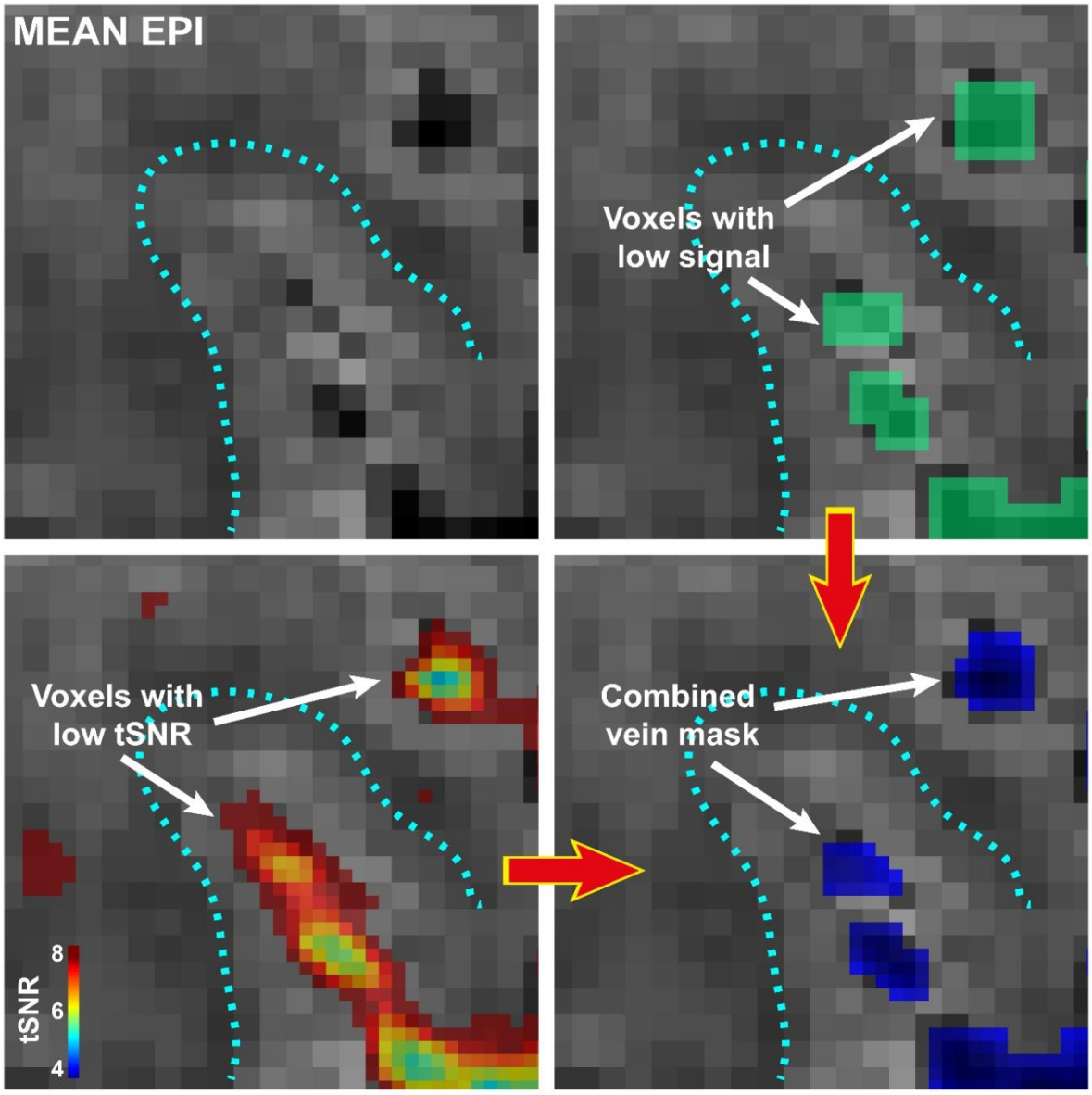

The venous voxels were identified with the following approach: (top-left) temporal mean of the functional EPI data was first computed using *fslmaths*, (top-right) voxels with low intensity were selected from the mean EPI image by setting an arbitrary threshold (in this case, <60 mean EPI signal) so as to not include any GM voxels partial volume with a neighboring low intensity voxel, (bottom-left) voxels with low tSNR were selected by setting a threshold (in this case, <8) that also excludes most GM voxels, (bottom-right) the

combined mask of venous voxels was computed by a union operation of the low intensity and low tSNR maps.

FIGURE S4: Depth-dependent analysis (Left) in anatomical space using the Conventional workflow, (Middle) in EPI space using MP2RAGE distorted using TOPUP and (Right) in EPI space using the MI-EPI workflow

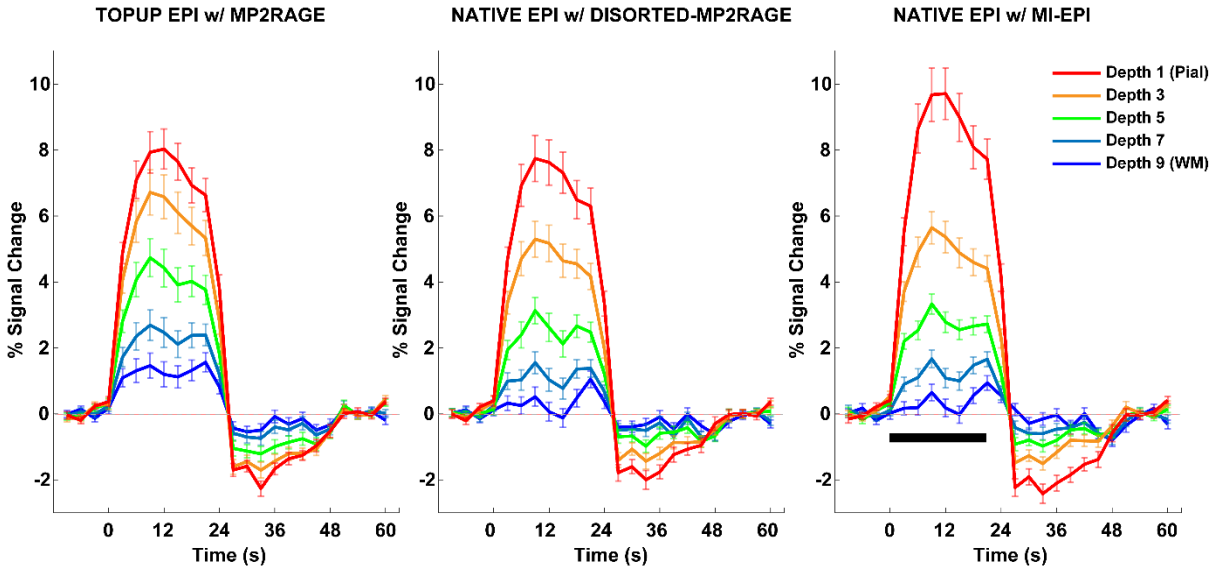

In Figure S4, the time-course obtained from the native EPI using distorted-MP2RAGE to define the cortical depths results in a similar dynamic range of the BOLD signal as using the MI-EPI, except the uppermost depth. As the difference between the middle and right panels is the definition of the cortical depths not the functional data, this difference can be attributed to errors in registration (mostly) at the CSF-GM boundary. In the case of the TOPUP EPI (Figure S4, left) however, the signal change in the deeper layers is still much larger than what we observed with both the MI-EPI (Figure S4, right) and the distorted-MP2RAGE (Figure S4, middle), indicating that this difference is most influenced by the distortion-correction process. Thus, the differences between the Conventional approach and the MI-EPI approach are mostly due to the distortion-induced blurring (in the Conventional approach) but misregistration can additionally impact the cortical depth profiles obtained.

FIGURE S5: Relative ROI size analysis by bootstrapping.

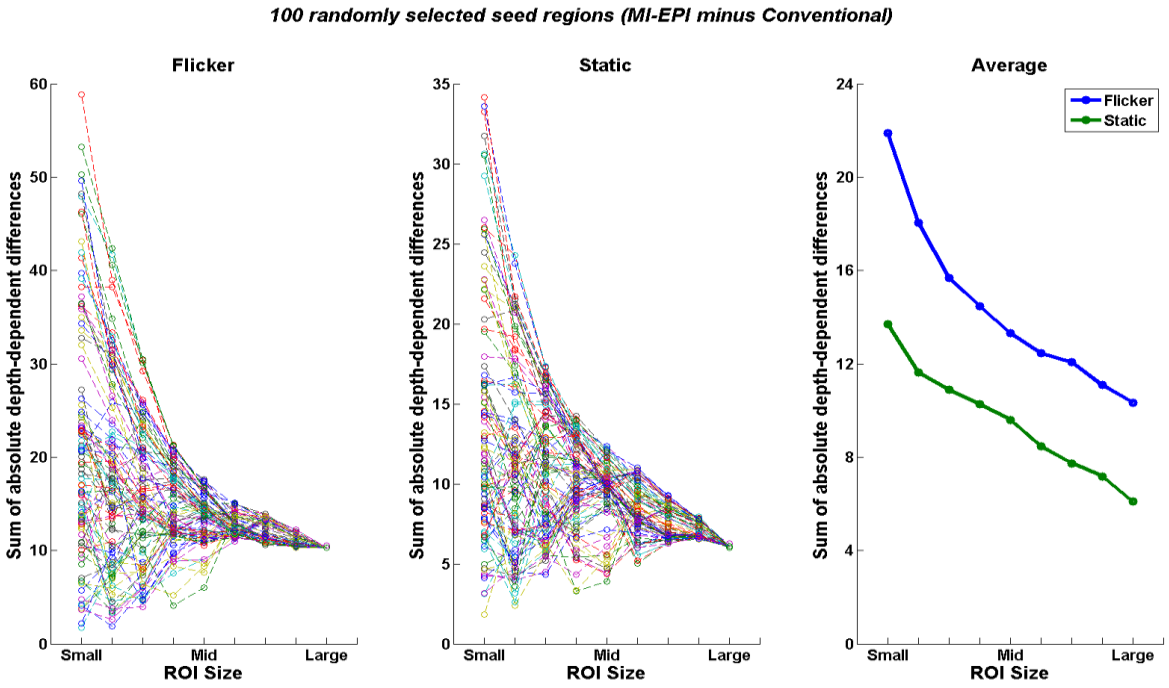

The seed voxel for the Relative ROI size analysis described in the manuscript was selected the maximum differential statistic for the two stimuli in the GLM. In order to examine if the choice of the seed region affected the observed slope in Figure 7, we repeated the same analysis but bootstrapped the seed voxel instead. For each seed region, the relative ROI size profiles i.e. the effect increasing the ROI size on the sum of the absolute depth-dependent differences of the PB signal between the MI-EPI workflow and the Conventional workflow for flicker and static stimulus conditions, respectively, are shown in Figure S5 (left and middle). The average of the 100 relative ROI size profiles for the two stimulus conditions (Figure S5, right). We observe that, similar to Figure 7, by increasing the ROI size (averaging more voxels around the seed ROI), the depth-dependent differences between workflows steadily decreases.